JOURNAL OF AGRICULTURAL AND FOOD CHEMISTRY

Influence of Epichlorohydrin Modification on Structure and Properties of Wheat Gliadin Films

YIHU SONG,*[,†,§] LINGFANG LI,[†] AND QIANG ZHENG[†,§]

Department of Polymer Science and Engineering, and Key Laboratory of Macromolecular Synthesis and Functionalization of Ministry of Education, Zhejiang University, Hangzhou 310027, China

The present study was to examine influence of epichlorohydrin (ECH) modification on structure and properties of glycerol-plasticized wheat gliadin films casting from ethanol/water (70/30 v/v) solution. The modified films were characterized using proton nuclear magnetic resonance (^{1}H NMR), Fourier transformation infrared (FTIR) spectra, dynamic mechanical analysis (DMA), and scanning electron microscopy (SEM). Water resistance (moisture absorption MA, water vapor permeability WVP, and weight loss in water WLW), tensile mechanical properties (Young's modulus E, tensile strength σ_b, and elongation at break ε_b), and thermal decomposition behavior were evaluated in relation to ECH content. Experimental results revealed that ECH modification gave rise to marked reduction in WLW and significant improvements in E and σ_b, which were accompanied by slight variations in MA, WVP, and thermal decomposition temperature. The improvements of E and σ_b were related to the formation of a partially cross-linked protein network even though the modification led to reductions in percentages of the hydrogen bonded NH groups and the β-sheet structure.

KEYWORDS: Wheat gliadin; modification; structure; properties

INTRODUCTION

Agricultural biofilms provide an opportunity to strengthen the agricultural economy and reduce consumption of petroleum and petroleum-based plastic package films. Wheat gluten has been considered as a class of renewable materials due to its abundant resource, low cost, unique viscoelastic properties, and good biodegradability (*1*). The gluten films are usually prepared via solution casting using water and/or ethanol as cosolvent (*2*). The films without plasticizer are brittle and are difficult to handle; thus a plasticizer such as glycerol is commonly used to lower the glass transition temperature and to increase chain mobility of proteins (*1*). Glycerol plasticization results in marked reduction in stiffness and strength performances, while it limits the application of protein-based biofilms (*3*).

Chemical or enzymic treatments have also been applied to modify wheat proteins as film forming materials (*4*−*6*). Reactive side groups of wheat proteins susceptible to various modifications make it possible to obtain three-dimensional protein networks with appropriate strength and functional properties (*7*). Dialdehydes and cysteine have been used to mediate the cross-linking of wheat proteins so as to improve water resistance and tensile strength and to lower water vapor permeability (WVP) of the casting films (*5*, *7*−*9*). Thermal treatment of the film forming solution or the resultant film significantly affects structure and properties of the final products (*10*).

Gliadins are important storage proteins that provide viscous character to wheat gluten (*11*). Gliadins are characterized by high contents of Gln, Pro, and Phe residues and are usually classified into four groups (α-, β-, γ-, and ω-gliadins). α-, β-, and γ-gliadins are major components containing intrachain disulfide bonds, whereas the ω-gliadins occur in much lower proportions lacking cysteine residue. Wheat gliadins have perfect film forming character (*8*). The cross-linking of proteins depends on the type of gliadins that ultimately affects the properties of films. We in this article modify wheat gliadins using epichlorohydrin (ECH) and prepare glycerol-plasticized gliadin films. The effects of ECH content on morphology, glass transition, mechanical properties, moisture absorption (MA), weight loss in water (WLW), and WVP of the modified gliadin films are investigated.

MATERIALS AND METHODS

Materials. Wheat gluten with protein content ≥75 wt %, ash content ≤0.95 wt %, and moisture content ≥9 wt % was supplied by Shanghai Wangwei Food Co. Ltd., China. Glycerol, ECH, and other chemicals were analytical grade reagents.

A total of 100 g of crude wheat gluten was dispersed in 500 mL of 70/30 (v/v) ethanol/water mixture, stirred at 25 °C for 12 h, and centrifuged at 4000 rpm for 15 min at room temperature. The resulting supernatant containing the gliadin-rich fraction was dried at room temperature and was further freeze-dried using a freeze-dryer (FD-1, Beijing Youde Techn. Develop. Co. Ltd., China). The dried gliadin-

* To whom correspondence should be addressed. E-mail: s_yh0411@zju.edu.cn.

[†] Department of Polymer Science and Engineering.

[§] Key Laboratory of Macromolecular Synthesis and Functionalization of Ministry of Education.

10.1021/jf802961b CCC: $40.75
Published on Web 03/02/2009

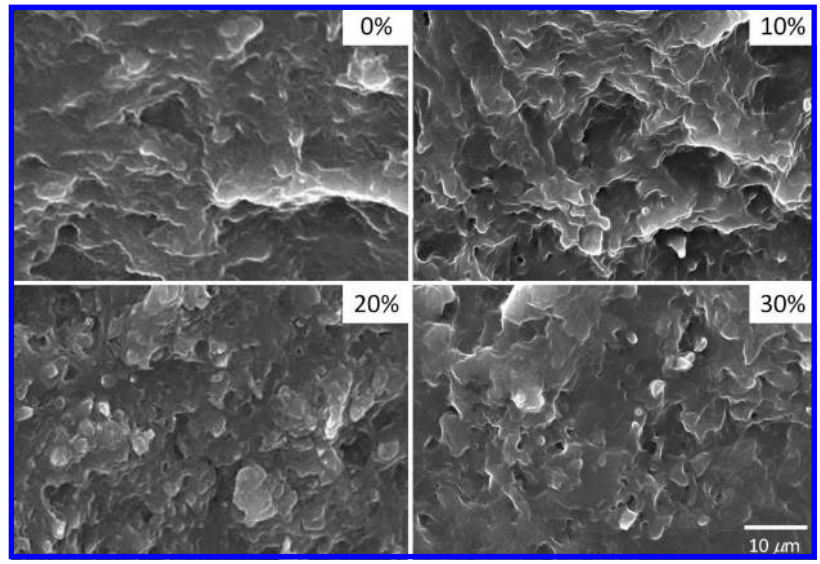

Figure 1. SEM micrograph of the films with different w_{ECH} as indicated.

rich fraction was ground to pass through 100 mesh sieve. The molecule weights of gliadins were ranged in 30−100 kDa as determined from sodium dodecyl sulfate−polyacrylamide gel electrophoresis analysis (*12*).

Film Formation. Freeze-dried gliadin powders were dissolved in 70/30 (v/v) ethanol/water mixture to yield a 10 wt % solution. Glycerol of 0.2 g/g dry protein was added into the solution, and the solution was heated with stirring at 50 °C for 30 min. ECH of 0−1.2 g/g dry protein was then added under gentle stirring until a transparent solution was formed. The mixture was reacted for another 30 min and was then cooled down to room temperature. The solution was poured onto plastic Petri dishes with an inner diameter of 90 mm and was dried at 50 °C for 72 h. The films were carefully detached and were stored in desiccators at 50% and 75% relative humidities (RH) until testing.

Film Thickness. Film thickness (*H*) was measured using a hand-held micrometer (Shanghai Measuring & Cutting Tool Works, China). The *H* values were reported as means of nine measurements from different locations of each product.

Morphology Observation. The samples were stretched to break at room temperature. Morphology of the fracture surface was observed after coating with gold using a scanning electron microscope (SEM) (SLR10N, FEI, The Netherlands) at 25 kV.

Proton Nuclear Magnetic Resonance (^{1}H NMR) Measurement. Soluble ^{1}H NMR spectra were measured on a Bruker ARX 500 spectrometer using dimethylsulfoxide-d_6 as solvent and tetramethylsilane (TMS) as internal standard.

Fourier Transformation Infrared (FTIR) Spectra Measurement. The gliadin solution was coated on potassium bromide plate and was dried under ultraviolet lamp radiation. FTIR spectra were measured using VECTOR 22 FI-IR spectrometer with a resolution of 4 cm^{-1}.

Dynamic Mechanical Analysis (DMA). DMA was performed at 1 Hz with a dynamic mechanical thermal analyzer (DMA 242, NETZSCH, Germany) using tensile mode at a heating rate of 3 °C min^{-1}. Paraffine oil was coated on the sample surface in order to eliminate moisture interchange between the sample and the surroundings.

Moisture Absorption (MA) Test. Triplicate specimens of 0.5 g were stored for 1 week until constant weight in an airtight desiccator at 23 °C over anhydrous phosphorus pentoxide (P_2O_5). The predried samples were transferred into desiccators at 70% RH and were stored for 72 h at room temperature to constant weight. MA was evaluated on a dry basis and was reported as the average of three replicates.

Water Vapor Permeability (WVP) Test. WVP of films was determined gravimetrically at 20 °C according to ASTM E96-80 (1983) with a slight modification. The predied films were mechanically sealed to glass test cups containing P_2O_5 (0% RH). The exposed area of the test cup was 0.0243 m^2. The cups were placed in airtight desiccators maintained at 70% RH. WVP was determined after steady-state condition was reached where the weight gain became constant over the prescribed time interval. WVP was calculated according to WVP $= wH/A_e t\Delta p$ (*13*). Here, A_e is the area of exposed film, Δp is the vapor pressure across the film, and w is the weight gain of the cup over the prescribed time interval t.

Weight Loss in Water (WLW). Triplicate predried films of 10 × 50 mm were immersed in 300 mL of deionized water at 25 °C for 48 h with occasional gentle manual agitation. Deionized water was changed twice everyday to avoid microbial growth. The undissolved matter was dried over P_2O_5 at 25 °C in the desiccator until constant mass. WLW was calculated according to dry mass before and after immersing (*8*).

Tensile Test. Tensile testing was performed on a universal testing machine (CMT-4204, Shenzhen SANS Test Machine Co. Ltd., China) with an extension rate of 20 mm min^{-1} at 25 °C. Young's modulus (E), tensile strength (σ_b), and elongation at break (ε_b) were evaluated from five duplicates for each product.

Thermogravimetric Analysis (TGA) Test. TGA was carried out under an air atmosphere in a Pyris 6 thermogravimetric analyzer (Perkin-Elmer) with a heating rate of 10 °C min^{-1}. The samples were predried over P_2O_5 in the desiccators for 1 week before test.

Statistical Analyses. Statistical analyses were performed using OriginPro 7.50 software (OriginLab Co., Northampton, USA). A one-way analysis of variance (ANOVA) followed by a Tukey test ($P < 0.05$) was used to identify whether the differences between the treatments were significant.

RESULTS AND DISCUSSION

Morphology. Figure 1 shows SEM micrographs taken at the tensile break surface of the films modified with different ECH. The unmodified gliadin film and the film modified with weight content of ECH (w_{ECH}) of 10 wt % exhibit characteristics of tough fracture with delamination and corrugation. The delamination becomes less significant in the films with higher ECH contents. Spherulite-like domains with a size less than 2 μm appear as the main character in the fracture surface of the films with $w_{ECH} = 20$ wt % and $w_{ECH} = 30$ wt %. At large quantities of ECH used, the modification introduces additional chemical cross-linking bonds among gliadin chains, which alters the miscibility between glycerol and gliadins and causes gliadins to aggregate into the spherulite-like domains.

^{1}H NMR and FTIR Spectra. Figure 2 shows ^{1}H NMR spectra of the pristine and the modified gliadins. The peak at a chemical shift of 2.5 ppm is due to resonance of residual protons in DMSO-d_6. The peak at 7.9 ppm can be assigned to backbone NH protons arising from Gln and Phe residues, while the

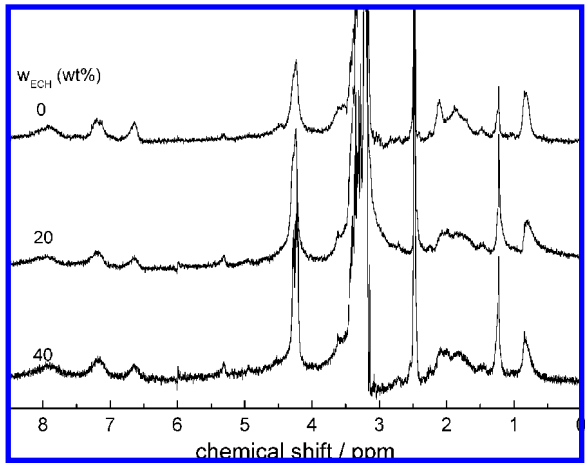

Figure 2. ^{1}H NMR spectra of the films with different w_{ECH}.

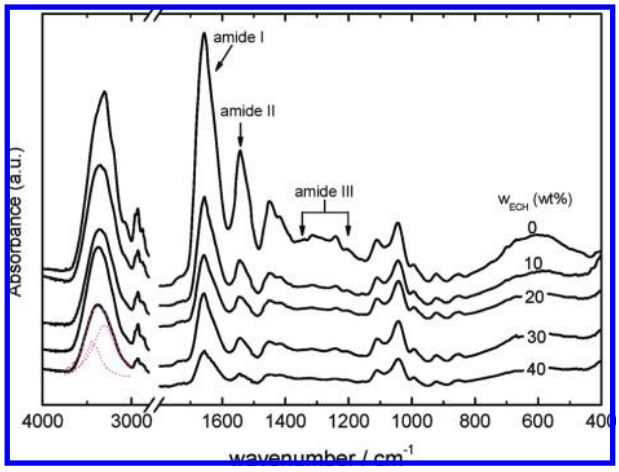

Figure 3. FTIR spectra of the films with different w_{ECH}. The dashed curve shows the absorbance profile in the NH stretching vibration region calculated according to Lorentzian line-shape fitting and the dotted curves show the calculated single components peaked at 3300 and 3450 cm^{-1}, respectively.

features at 6.5 and 7.2 ppm correspond to protons of Gln side-chain amine groups as well as aromatic Tyr protons (*14*). The peak at 4.2 ppm is due to the major contribution from the α protons of the main amino acid Gln together with minor contributions from the α protons of Arg and Glu. The strong peak at 3.2 ppm can be assigned to the Phe β resonance and the weak shoulder peak at 3.6 ppm arises mainly from the Gly α protons coupled with the Pro δ site resonance. The doublet situated in the 1.5−2.4 ppm region arises from overlapped β and γ resonances from aliphatic side-chains of the main amino acids of Pro and Gln. The two isolated singlets at 1.2 ppm and 0.8 ppm are due to -CH_2- and -CH_3 protons from side chains of mobile minor amino acids (Leu, Thr, Ala, and Arg). As shown in **Figure 2**, the chemical modification does not influence the peak positions in the ^{1}H NMR spectra. However, it causes a significant increase in intensity of the -CH_2- peak (1.2 ppm) and a reduction in intensity of the Gln side chain amine proton peaks (6.5 and 7.2 ppm) with respect to the -CH_3 peak (0.8 ppm), revealing the occurrence of chemical reaction between ECH and gliadins. ECH reaction with proteins has been revealed in extruded corn meal (*15*).

Figure 3 shows FTIR spectra. The broadband in the 3600−3000 cm^{-1} range can be assigned to N−H stretching vibration and the bands at 2980−2850 cm^{-1} correspond to the characteristic C−H stretching of the -CH_2- and -CH_3 groups of

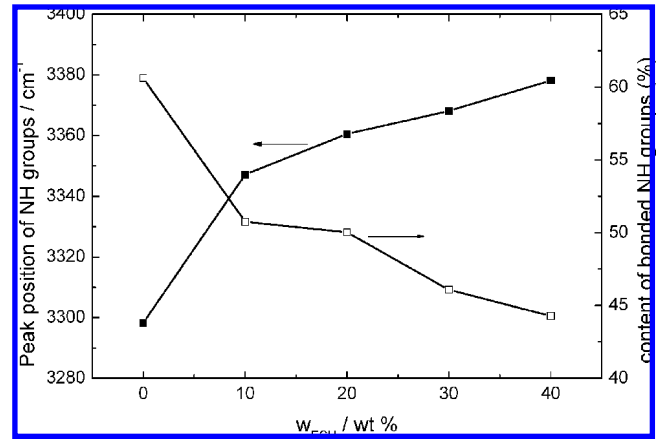

Figure 4. Peak position of the N−H stretching vibration and the content of hydrogen bonded NH group in the films with different w_{ECH}.

saturated structures (*16*). The absorption bands at 1750−1580 cm^{-1}, 1580−1480 cm^{-1}, and 1370−1150 cm^{-1} are related to amide I (80% C═O stretch, 10% C−N stretch, and 10% N−H bend), amide II (60% N−H bend and 40% C−N stretch), and amide III (40−60% N−H in-plane bend and 18−40% C−N stretch coupled with C−H and N−H deformation), respectively (*17*). The ECH modification does not introduce new absorbance bands. In particular, the characteristic peaks of epoxy group (915 cm^{-1}) and C−Cl bond (723−747 cm^{-1}) are absent in the modified gliadins. ECH can react with hydroxyl, amino, and carboxyl groups of amino acid residues so as to cross-link gliadins with the formation of -CH_2-CH(OH)-CH_2- linkage. At high ECH contents, side reactions such as ECH homopolymerization may also take place, which, however, could not be distinguished from ^{1}H NMR and FTIR spectra.

The peak position of the N−H stretching vibration is shifted toward high wavenumbers with increasing w_{ECH}, as shown in **Figure 4**. The N−H stretching absorbance bands were decomposed into two single peaks centered at 3300 and 3450 cm^{-1} assigned to the hydrogen bonded and the free NH groups, respectively. The dotted curves in **Figure 3** show the calculated single components in the N−H stretching region to the film of w_{ECH} = 40 wt %. The area absorbances of the single components at 3300 and 3450 cm^{-1}, A_{3300} and A_{3450}, were used to estimate the percentage of the hydrogen bonded NH groups according to $A_{3300}/(A_{3300} + A_{3450})$ and the result is shown in **Figure 4**. The chemical modification causes a reduction in percentage of the hydrogen bonded NH groups, from 61% to 44% as increasing w_{ECH} from 0 wt % to 40 wt %.

ECH modification hardly influences the peak position of the amide I and amide II absorption, while it causes several variations in the spectra of the amide III region. The better defined amide III bands are quite suitable for determination of α-helix (1330−1295 cm^{-1}), β-turn (1295−1270 cm^{-1}), random coil (1270−1255 cm^{-1}), and β-sheets (1245−1220 cm^{-1}) structures (*18*). **Figure 5** shows the FTIR spectra and the inverted second derivative spectra in the amide III region. The unmodified film exhibits four absorption peaks at 1340, 1314, 1285, and 1240 cm^{-1}, respectively. In the chemically modified films, the 1340 cm^{-1} peak disappears, while three peaks at 1355, 1345, and 1333 cm^{-1} appear in the α-helix region. The band at 1314 cm^{-1} is shifted to higher wavenumbers with increasing w_{ECH}. The inverted second derivative spectra disclose a peak at 1303 cm^{-1}, whose intensity becomes strong in the modified films. Therefore, the chemical modification causes marked conformation change in the α-helix structure of gliadins. Besides, the chemical modification causes the band at 1287 cm^{-1}

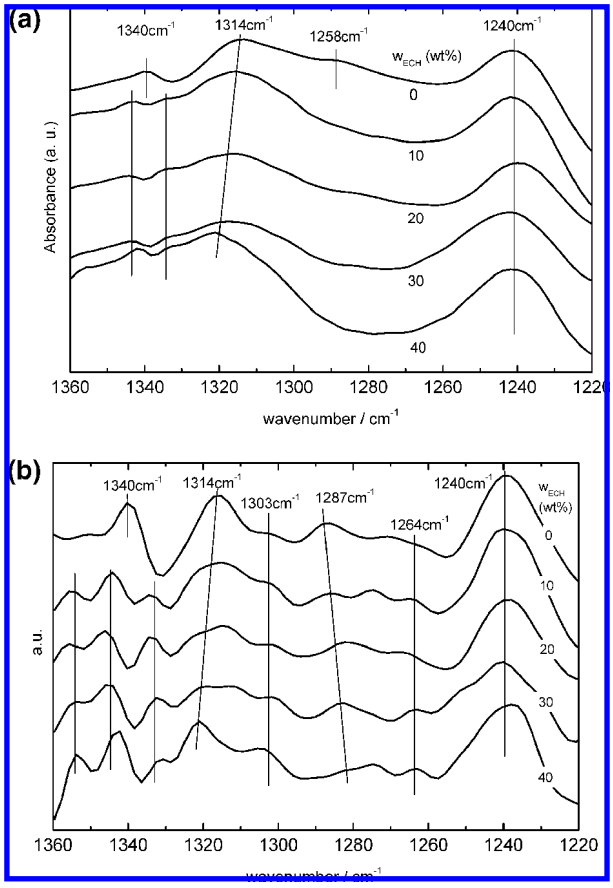

Figure 5. FTIR spectra (a) and inverted second derivative spectra (b) of the films in the amide III region.

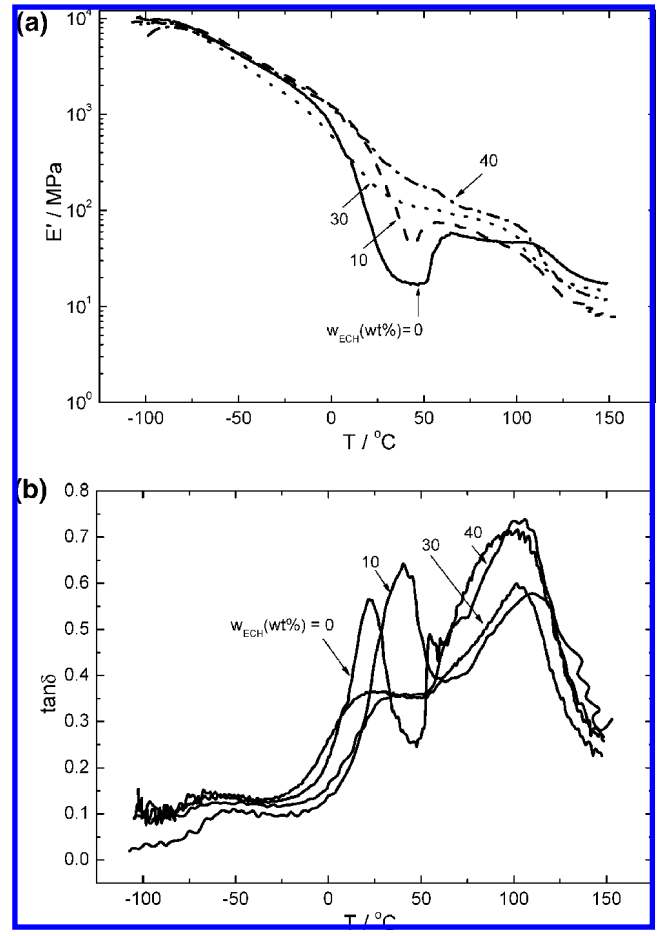

Figure 6. Effect of w_{ECH} on storage modulus E' (a) and loss factor tan δ (b) of the films.

(β-turn) to shift toward lower wavenumbers and the intensity of the band at 1264 cm^{-1} (random coil) to increase markedly. The chemical modification does not influence the position of the 1240 cm^{-1} (β-sheets) band. However, the absorbance ratio A_{1240}/A_{1656} is reduced from 0.055 of the unmodified film to 0.042, 0.038, 0.041, and 0.038 for the films with w_{ECH} of 10, 20, 30, and 40 wt %, respectively. The spectra in the amide III region reveal that the percentage of the β-sheet structure decreases considerably after chemical modification, which is accompanied by an increment in the percentage of random coiled structure.

DMA. Figure 6 shows storage modulus (E') and loss factor (tan δ) as a function of temperature (T) for the films. With increasing T, the samples traverse the glassy region, the transition region (tan δ peak and E' drop), and the rubbery plateau in sequence. A characteristic decrease of 3 orders of magnitude in E' is observed at the broad glass-to-rubber transition. Drying at 50 °C for 3 days leads to modification of the gliadin structure in the absence of ECH, which is due to the formation of disulfide intermolecular cross-links (*19*). The unmodified gliadin film exhibits an obvious increase in E' with increasing T from 50 to 64 °C, revealing that the cross-linking reaction between gliadin molecules is not complete in the condition investigated. The denaturation temperature of gliadins at 58 °C (*19*) could well account for the E' increment in **Figure 6a**. The cross-linking reaction causes the gluten viscosity to increase upon heating above 55 °C (*20*), which is accompanied by significant drops in the amount of free sulfhydryl groups and sodium dodecyl sulfate extractability (*21*). With the increase in T from 64 to 109 °C, E' decreases very slightly due to canceling of thermally agitated softening and the cross-linking reaction. The E' increment in the film with w_{ECH} = 10 wt % is less marked as that of the unmodified gliadin film. The E' increment can still be observed from 43 to 54 °C, suggesting that 10 wt % ECH modification at 50 °C for 3 days does not consume away all the active chemical groups of gliadins without addition of a catalyst. The films with w_{ECH} = 30 and 40 wt % do not exhibit E' increment upon heating. The results suggest that the modification at large ECH contents results in full intermolecular cross-linking during the film formation at 50 °C and heating the films of w_{ECH} = 30 and 40 wt % during the DMA tests does not lead to further cross-linking reaction.

As observed in **Figure 6b**, the tan δ curve of the unmodified gliadin film shows a very weak transition peak at −67.3 °C and two strong transitions peaked at 22.0 and 101.9 °C, respectively. The E' increment corresponds to a shoulder peak at 54.0 °C. The low temperature transition at −67.3 °C is likely associated with a glass transition temperature (T_g) of the glycerol-rich phase (*22*). The two high temperature peaks reflect the α-transition or glass transition of the gliadin-rich phase, which is broken down by the cross-linking reaction occurred during DMA test. The two glass transition temperatures of the gliadin-rich phase are lower than those of unplasticized gliadins at 124−145 °C (*23*). In the film of w_{ECH} = 10 wt %, these two glass transition temperatures are shifted to higher temperatures due to chemical cross-linking. In the films with w_{ECH} = 30 and 40 wt %, the middle peak becomes inconspicuous, which is consistent with the continuous decrease in E' in the same temperature region. Our previous study revealed that wheat gluten bioplastic compression molded at temperatures below 105 °C show two subglass transitions assigned to the gluten-rich phase while the low temperature transition at about 20∼35

Table 1. Influence of w_{ECH} on H, MA, WVP, and WLW of the Films[a]

w_{ECH}/wt %	H/μm	MA/wt %	WVP/10^{-11} g m^{-1} s^{-1} Pa	WLW/wt %
0	200 ± 20^{a}	15.8 ± 0.1^{c}	67.4 ± 2.4^{a}	34.1 ± 3.7^{a}
10	160 ± 15^{b}	15.8 ± 0.2^{c}	66.4 ± 2.7^{b}	27.6 ± 3.8^{b}
20	154 ± 22^{c}	15.8 ± 0.2^{c}	66.6 ± 3.4^{b}	23.5 ± 3.6^{c}
30	$148 \pm 11^{d,e}$	16.1 ± 0.1^{b}	65.6 ± 3.5^{c}	$22.4 \pm 3.6^{c,d}$
40	$138 \pm 11^{e,f}$	16.2 ± 0.1^{b}	65.3 ± 2.8^{c}	22.0 ± 3.8^{d}
50	144 ± 17^{e}	16.5 ± 0.1^{a}	65.5 ± 3.1^{c}	

[a] Means followed by different letters in the same column are significantly different ($P < 0.05$).

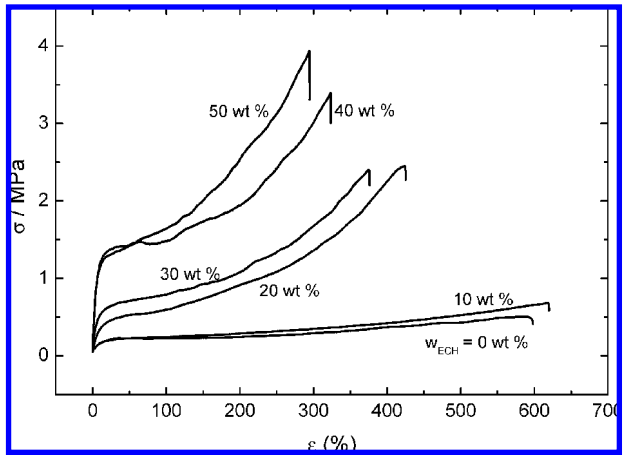

Figure 7. Effect of w_{ECH} on stress−strain ($\sigma-\varepsilon$) behavior of the films.

°C becoming inconspicuous in the sample molded at 125 °C (*24*). The DMA curves in **Figure 6** prove the occurrence of cross-linking reaction between ECH and gliadins during film formation.

Water Resistance. Table 1 shows influence of w_{ECH} on H, MA, WVP and WLW of the films. H decreases markedly with increasing w_{ECH} ($P < 0.05$), which could be ascribed to the diluting effect of ECH to gliadins in the casting solution. MA increases while WVP decreases very slightly with increasing w_{ECH} ($P < 0.05$). The reduction of WVP with respect to w_{ECH} might be due to the thickness effect (*25*). All the films maintain their integrity in water, while the ECH modification causes a significant reduction in WLW ($P < 0.05$), from WLW = 34.1 wt % to WLW = 22.0 wt % with increasing w_{ECH} from 0 to 40 wt %. The WLW value of the film at w_{ECH} = 0 wt % corresponds to protein solubility (soluble gliadin fraction by the gliadin fraction in the film) of 20.9 wt %, revealing a partially cross-linked network in the film formed at 50 °C. The solid solubility (fraction of soluble mater except for glycerol by the total fraction of gliadins and ECH in the film) is estimated as 14.8, 11.7, 12.2, and 13.3 wt %, respectively, for the films with w_{ECH} of 10, 20, 30, and 40 wt %. The slight increase in solid solubility at $w_{ECH} \geq 30$ wt % might indicate the formation of ECH homopolymers during the film preparation. In contrary to aldehyde cross-linking of gliadin that results in marked reduction in WVP (*7*), the variation of WVP with respect to ECH content is considerably small. The results in **Table 1** reveal that the ECH modification introduces additional cross-linking sites among gliadin macromolecules while it hardly influences the hydrophilicity of the resultant films.

Tensile Mechanical Properties. Figure 7 shows the influence of w_{ECH} on stress−strain ($\sigma-\varepsilon$) relationship of the gliadin films after equilibrating at 75% RH. The films show yielding-like deformation where σ increases rapidly at small strains but very slowly after yielding. At the same ε level, σ increases markedly with w_{ECH}. The deformation after yielding exhibits

Table 2. Influence of w_{ECH} on Mechanical Properties of the Films[a]

	70% RH			50% RH		
w_{ECH}/wt %	E/MPa	σ_b/MPa	ε_b (%)	E/MPa	σ_b/MPa	ε_b (%)
0	2.2 ± 0.4^{e}	0.71 ± 0.48^{f}	515 ± 108^{a}	28.8 ± 1.4^{e}	2.93 ± 0.28^{e}	241 ± 13^{c}
10	$2.1 \pm 0.4^{e,f}$	1.36 ± 1.12^{e}	406 ± 106^{b}	31.0 ± 1.8^{d}	4.31 ± 0.14^{d}	$243 \pm 1^{b,c}$
20	4.0 ± 0.8^{d}	2.01 ± 0.39^{d}	284 ± 69^{c}	33.6 ± 3.4^{c}	5.30 ± 0.15^{c}	229 ± 7^{d}
30	13.0 ± 1.2^{c}	2.85 ± 0.40^{c}	$240 \pm 52^{d,e}$	42.7 ± 0.8^{b}	6.16 ± 0.24^{b}	243 ± 8^{b}
40	21.2 ± 0.9^{b}	3.34 ± 0.29^{b}	$238 \pm 42^{e,f}$	44.4 ± 1.2^{a}	6.47 ± 0.63^{a}	250 ± 8^{a}
50	30.4 ± 1.8^{a}	3.66 ± 0.60^{a}	241 ± 40^{d}			

[a] Means followed by different letters in the same column are significantly different ($P < 0.05$).

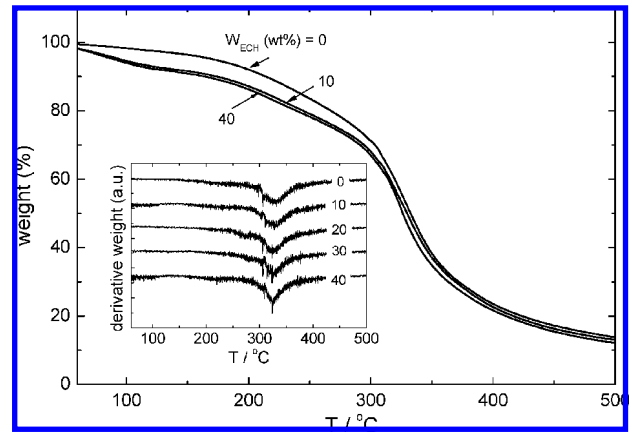

Figure 8. TGA traces of the films with different w_{ECH}. The inlet shows DTA curves of the films.

strain hardening as observed as an increase in the slope of the postyield region of the $\sigma-\varepsilon$ curve. The strain hardening becomes significant with increasing w_{ECH}, appearing as a characteristic of cross-linked gliadin network (*7*).

A small fraction of ECH (below 0.4 parts) has been used to cross-link extruded soy protein sheets to improve the strength and modulus performance (*26*). Aldehyde modification gives rise to stiffer gliadin films with improved fracture stress and reduced extensibility, while aldehyde concentrations above 1 wt % do not have any additional effect on mechanical properties (*7*). **Table 2** shows influence of w_{ECH} on E, σ_b, and ε_b of the films at 75% and 50% RH, respectively. It is found the mechanical properties are highly dependent on RH. The E and σ_b values at 50% RH are much higher than the respective values at 75% RH ($P < 0.05$). The ε_b value at 75% RH is higher than that at 50% RH at $w_{ECH} < 20$ *wt* % ($P < 0.05$). On the other hand, RH does not influence ε_b at $w_{ECH} > 30$ *wt* % ($P > 0.05$). At two humidities, E and σ_b increase significantly with increasing w_{ECH} up to w_{ECH} = 40 wt % ($P < 0.05$). The variation of ε_b with respect to w_{ECH} is highly dependent on RH. At 75% RH, ε_b decreases significantly with increasing w_{ECH} up to 30 wt % ($P < 0.05$). Further increasing w_{ECH} does not influence ε_b markedly ($P > 0.05$). At 50% RH, ε_b does not vary significantly with respect to w_{ECH} ($P > 0.05$). Improvement in σ_b of gliadin film formed under higher drying temperatures has been assigned to increases in the amount of hydrogen bonded β-sheets aggregates and in density of disulfide cross-links (*27*). In the ECH modified films, on the other hand, the mechanical properties are mainly related to increase in cross-linking density rather than the amount of the β-sheet structure.

TAG. Figure 8 shows TGA curve of the films in the T range from 60 to 500 °C and the inlet shows derivative thermogravimetric analysis (DTA) curves of the films with

various w_{ECH}. Increasing w_{ECH} from 10 wt % to 40 wt % only causes slight changes in the TGA curves so that only the TGA curves of the films modified with 10 wt % and 40 wt % ECH are shown. The unmodified gliadin film exhibits a three-stage decomposition during thermal degradation in oxidative atmosphere (*28*). The first stage at $T < 170$ °C corresponds to the water loss and the second stage at 170 °C $< T <$ 290 °C is assigned to glycerol evaporation and WG degradation. The third stage starting from 290 °C is involved in oxidation of the partially decomposed protein residues. The modified gliadin films show a weight loss faster than the unmodified gliadin film at $T < 120$ °C, which could be related to the evaporation of water and residual ECH. The ECH modification may not influence the weight loss in the second stage, while it shifts the decomposition temperature in the third stage to low temperatures. The protein decomposition peak temperature is located at 330.6 °C for the unmodified gliadin film, while it is shifted to 328.8, 325.6, 324.3, and 323.0 °C for the films with w_{ECH} of 10 wt %, 20 wt %, 30 wt %, and 40 wt % ECH, respectively, as shown in the DTA curves in the inlet. The chemical modification therefore leads to a slight degeneration in thermal decomposition of the film.

In summary, ECH modification causes marked reduction in WLW and significant improvements of E and σ_b of the gliadin film, which are accompanied with slight variations in MA, WVP and thermal decomposition temperature. FTIR spectra reveal that the chemical modification leads to reductions in percentages of the hydrogen bonded NH groups and the β-sheet structure. The improvement of E and σ_b with respect to w_{ECH} can be assigned to the formation of a partially cross-linked protein network resulting from the chemical reaction between ECH and gliadins as revealed from ^{1}H NMR and DMA studies.

ABBREVIATIONS USED

$\sigma-\varepsilon$, stress−strain; ε_b, elongation at break; σ_b, tensile strength; Δp, vapor pressure across the film; ^{1}H NMR, proton nuclear magnetic resonance; A_e, area of exposed film; DMA, dynamic mechanical analysis; DMSO-d_6, dimethylsulfoxide-d_6; DTA, derivative thermogravimetric analysis; E', storage modulus; E, Young's modulus; ECH, epichlorohydrin; FTIR, Fourier transformation infrared; H, film thickness; MA, moisture absorption; P_2O_5, phosphorus pentoxide; RH, relative humidity; T, temperature; t, time; tan δ, loss factor; T_g, glass transition temperature; TGA, thermogravimetric analysis; w, weight gain; w_{ECH}, weight content of ECH; WLW, weight loss in water; WVP, water vapor permeability.

ACKNOWLEDGMENT

This work was supported by the National Natural Science Foundation of China (50773068) and Natural Science Foundation of Zhejiang Province (Y407011).

LITERATURE CITED

(1) Jerez, A.; Partal, P.; Martinez, I.; Gallegos, C.; Guerrero, A. Rheology and processing of gluten based bioplastics. *Biochem. Eng. J.* **2005**, *26*, 131–138.

(2) Heralp, T. J.; Gnanasambandam, R.; McGuire, B. H.; Hachmeister, K. A. Degradable wheat gluten films: preparation, properties and applications. *J. Food Sci.* **1995**, *60*, 1147–1150.

(3) John, J.; Bhattacharya, M. Properties of reactively blended soy protein and modified polyesters. *Polym. Int.* **1999**, *48*, 1165–1172.

(4) Hernandez-Munoz, P.; Kanavouras, A.; Ng, P. K. W.; Gavara, R. Development and characterization of biodegradable films made from wheat gluten protein fractions. *J. Agric. Food Chem.* **2003**, *51*, 7647–7654.

(5) Hernandez-Munoz, P.; Villalobos, R.; Chiralt, A. Effect of cross-linking using aldehydes on properties of glutenin-rich films. *Food Hydrocolloid* **2004**, *18*, 403–411.

(6) Rayas, L. M.; Hernandez, R. J.; Ng, P. K. W. Development and characterization of biodegradable/ edible wheat protein films. *J. Food Sci.* **1997**, *62*, 160–162,189.

(7) Hernandez-Munoz, P.; Kanavouras, A.; Lagaron, J. M.; Gavara, R. Development and characterization of films based on chemically cross-linked gliadins. *J. Agric. Food Chem.* **2005**, *53*, 8216–8223.

(8) Hernandez-Munoz, P.; Kanavouras, A.; Villalobos, R.; Chiralt, A. Characterization of biodegradable films obtained from cysteine-mediated polymerized gliadins. *J. Agric. Food Chem.* **2004**, *52*, 7897–7904.

(9) Hernandez-Munoz, P.; Lopez-Rubio, A.; Del-Valle, V.; Almenar, E.; Gavara, R. Mechanical and water barrier properties of glutenin films influenced by storage time. *J. Agric. Food Chem.* **2004**, *52*, 79–83.

(10) Roy, S.; Weller, C. L.; Gennadios, A.; Zeece, M. G.; Testin, R. F. Physical and molecular properties of wheat gluten films cast from heated film-forming solutions. *J. Food Sci.* **1999**, *64*, 57–60.

(11) Wieser, H. Chemistry of gluten proteins. *Food Microbiol.* **2007**, *24*, 115–119.

(12) Sun, S.; Song, Y.; Zheng, Q. PH-induced rheological changes for semi-dilute solutions of wheat gliadins. *Food Hydrocolloid.* **2008**, *22*, 1090–1096.

(13) Letendre, M.; D'Aprano, G.; Lacroix, M.; Salmieri, S.; St-Gelais, D. Physicochemical properties and bacterial resistance of biodegradable milk protein films containing agar and pectin. *J. Agric. Food Chem.* **2002**, *50*, 6017–6022.

(14) Alberti, E.; Humpfer, E.; Spraul, M.; Gilbert, S. M.; Tatham, A. S.; Shewry, P. R.; Gil, A. M. A high resolution 1H magic angle spinning NMR study of high-M_r subunit of wheat glutenin. *Biopolymers.* **2001**, *58*, 33–45.

(15) Kojima, M.; Hanna, M. A.; Gennadios, A. Water solubility and macromolecular properties of corn meal extrudates as affected by epichlorohydrin. *Cereal Chem.* **1997**, *74*, 526–529.

(16) Nanda, P. K.; Rao, K. K.; Nayak, P. L. Biodegradable polymers. XI. Spectral, thermal, morphological, and biodegradability properties of environment-friendly green plastics of soy protein modified with thiosemicarbazide. *J. Appl. Polym. Sci.* **2007**, *103*, 3134–3142.

(17) Robertson, G. H.; Gregorski, K. S.; Cao, T. K. Changes in secondary protein structures during mixing development of high absorption (90%) flour and water mixtures. *Cereal Chem.* **2006**, *83*, 136–142.

(18) Cai, S. W.; Singh, B. R. Identification of β-turn and random coil amide III infrared bands for secondary structure estimation of proteins. *Biophys. Chem.* **1999**, *80*, 7–20.

(19) Leon, A.; Rosell, C. M.; de Barber, C. B. A differential scanning calorimetry study of wheat proteins. *Eur. Food Res. Technol* **2003**, *217*, 13–16.

(20) Hayta, M.; Alpaslan, M. Effects of processing on biochemical and rheological properties of wheat gluten proteins. *Nahrung* **2001**, *45*, 304–308.

(21) Lagrain, B.; Brijs, K.; Veraverbeke, W. S.; Delcour, J. A. The impact of heating and cooling on the physico-chemical properties of wheat gluten-water suspensions. *J. Cereal Sci.* **2005**, *42*, 327–333.

(22) Sun, S. M.; Song, Y. H.; Zheng, Q. Morphologies and properties of thermo-molded biodegradable plastics based on glycerol-plasticized wheat gluten. *Food Hydrocolloid* **2007**, *21*, 1005–1013.

(23) Noel, T. R.; Parker, R.; Ring, S. G.; Tatham, A. S. The glass-transition behaviour of wheat gluten proteins. *Int. J. Biol. Macromol.* **1995**, *17*, 81–85.

(24) Sun, S. M.; Song, Y. H.; Zheng, Q. Thermo-molded wheat gluten plastics plasticized with glycerol: Effect of molding temperature. *Food Hydrocolloid* **2008**, *22*, 1006–1013.

(25) Kristo, E.; Biliaderis, C. G.; Zampraka, A. Water vapour barrier and tensile properties of composite caseinate-pullulan films: Biopolymer composition effects and impact of beeswax lamination. *Food Chem.* **2007**, *101*, 753–764.
(26) Zhang, J.; Mungara, P.; Jane, J. Mechanical and thermal properties of extruded soy protein sheets. *Polymer* **2001**, *42*, 2569–2578.
(27) Mangavel, C.; Barbot, J.; Popineau, Y.; Gueguen, J. Evolution of wheat gliadins conformation during film formation: A Fourier transform infrared study. *J. Agric. Food Chem.* **2001**, *49*, 867–872.
(28) Tunc, S.; Angellier, H.; Cahyana, Y.; Chalier, P.; Gontard, N.; Gastaldi, E. Functional properties of wheat gluten/montmorillonite nanocomposite films processed by casting. *J. Membr. Sci.* **2007**, *289*, 159–168.

Received for review September 23, 2008. Revised manuscript received November 25, 2008. Accepted November 25, 2008.

JF802961B